AIMS Mathematics, 7(4): 7012–7025.
DOI: 10.3934/math.2022390
Received: 10 November 2021
Revised: 26 December 2021
Accepted: 10 January 2022
Published: 07 February 2022

http://www.aimspress.com/journal/Math

Research article

An alternative opportunity of future Psyche mission using differential evolution and gravity assists

Vijil Kumar[1,*], **Badam Singh Kushvah**[1] **and Mai Bando**[2]

[1] Department of Mathematics and Computing, Indian Institute of Technology (ISM), Dhanbad 826004, Jharkhand, India

[2] Department of Aeronautics and Astronautics, Kyushu University, 744 Motooka, Nishi-Ku, Fukuoka 819-0395, Japan

* **Correspondence:** Email: vijilchoudhary@gmail.com; Tel: +919058037688.

Abstract: NASA's Psyche mission will launch in August 2022 and begin a journey of 3.6 years to the metallic asteroid: Psyche, where it will orbits and examine this unique body. This paper presents an alternative opportunity of the Psyche mission as well as the return opportunity to the Earth. It uses Mars's gravity assists to rendezvous with and orbits to the largest metal asteroid in the solar system. The spacecraft orbits around Psyche for approximately 1710 solar days, then starts its return journey. In the outer layer of the proposed methodology, the differential evolution algorithm is used to find the optimal launch, flyby and arrival date. In the inner layer, Lambert's algorithm is used for finding the feasible and optimal space trajectories solution. Considering gravity assists, before the gravity assists impulse, an optimal thrust impulse has been calculated at periapsis of the fly-by planet that gives the maximum Δv_2 to the spacecraft.

Keywords: Psyche asteroid mission; differential evolution algorithm; Lambert's problem; transfer trajectory
Mathematics Subject Classification: 37N05, 65K05, 70F05, 70F15, 70M20

1. Introduction

NASA's first program, which began in 1972, demonstrated the scientific advantage that could be achieved from a cost-capped, competitively awarded deep space exploration mission. Pioneer 10, which flew past an unidentified asteroid on August 2, 1972, was the first spacecraft to visit an unknown asteroid [1]. Then another, on October 18, 1988, the Galileo spacecraft was launched. It was the first spacecraft to send an entry probe into the atmosphere of an outer planet, in this case Jupiter's. On October 29, 1991, he made a flyby with the asteroid 951 Gaspra before entering Jupiter's parking

orbit [15]. Whereas, the Near Earth Asteroid Rendezvous-shoemaker mission was initialized on February 17, 1996. It was the first asteroid mission, with the probe orbiting the 433 Eros asteroid at a distance of about 50 kilometers. Following that, various asteroid missions to collect physical samples and return to Earth were launched, like Table 1.

Table 1. The successful asteroid mission.

Mission	Year	References
Sturdust	1996	[6]
Hayabusa	2003	[30]
Dawn	2007	[20]
Hayabusa2	2014	[25]
OSIRIX-REx	2016	[11]

The proposed project Psyche: journey to a metal world, handed by principal investigator Dr. Linda Elkins-Tontan of Arizona state university, was selected for implementation as a part of NASA's discovery exploration program in January 2017 [16]. The electric propulsion makes possible this mission and would use SPT-140 Hall-thrusters to rendezvous and orbit around Psyche, one of the largest asteroid in the solar system. It's the first time Hall-thrusters have been seen outside lunar orbit [8] and the references therein [13, 14, 23, 24].

Whereas, the two-point boundary value problem (TPBVP) in the two-body dynamical environment is known as Lambert's problem. It requires the positions of any two celestial bodies and the transfer time between them. The solution of the Lambert's problem gives the initial and final velocities of the transfer trajectory. A brief knowledge about Lambert's problem is given by Blanchard et al. [5]. They discussed various cases of Lambert's problem in to a single form. The research articles [3,9] have described related numerical work. It is a fundamental astrodynamics problem. Its solution may be used in a variety of orbit maneuver missions' guidance, control, and optimization procedures, including orbit transfer, orbit interception, and orbit rendezvous [32]. Furthermore, Battin [4] pointed out that in the two-point boundary value problem, the product of the chordal and radial terminal velocity components is constant. This characteristic may be utilized to address the challenge of determining the optimal free-time orbit movement between two fixed endpoints. The minimum-fuel solution for the single-impulse free-time problem is found by calculating the roots of a quadratic polynomial [4].

Whereas, the differential evolution algorithm (DEA) has been included in this methodology to found the optimal launch, flyby and arrival date [12, 31]. Most of the basic and advanced properties of the DEA are given by Uday K. Chakraborty in his book [7]. He described details of the DEA in the area of optimization research like advanced planning and scheduling model, real time task scheduling models, reliability optimization models, communication network model, multi-objective rendezvous model and many more [35]. It has been effectively applied in the trajectory optimization problem and it gives a better result compare to the Particle swarm optimization technique [10, 17]. The results of recent research suggests that the non-dominated sorting DEA can be effectively used to discover various optimal solution, the information on which could be helpful to the best optimal launch date of trajectory design [18]. Furthermore, [33, 34] developed a simplified approach for determining the minimum-fuel solution based on the minimum-fuel free-time solution by computing and comparing two candidates at most. In addition, the shooting technique [21], the homotopic approach [29], and

differential algebra [2] are used to solve the multiple-revolution perturbed Lambert's problem.

On the other hand, the interplanetary and interstellar missions frequently employ gravity assistance. Mariner 10, Pioneer 10, Pioneer 11, Voyager 1, Voyager 2, Galileo, Cassini, Rosetta and Messenger are just a couple of the missions that have employed gravity assists. The gravity-assist trajectories can achieve greater orbital energies than those previously feasible with simply chemical rocket propulsion, offering up new avenues for further exploration of our solar system [26]. The Mariner 10, Messenger, Cassini and Galileo missions used inner-planetary gravity assists to reach Mercury, Saturn and Jupiter, respectively. The Voyager and Pioneer missions used gravity assists to escape from the solar system. The design of interplanetary and interstellar missions presents considerable optimization difficulties. When the planetary gravity-assist order is changed, they become exceedingly nonlinear, with several significant discontinuities in the region of optimal solutions [27].

The pressure to reduce the cost of interplanetary missions has resulted in a greater emphasis on developing missions with shorter flight periods, smaller launch vehicles, and simpler flight systems in recent years [8, 18]. Because of their high propellant efficiency, these criteria have reignited interest in low-thrust propulsion systems. The majority of existing trajectory optimization software represents a sequence of discrete events: launch time, planetary flyby periods, and any deep space maneuvers that may be necessary [28]. In this regard, we proposed a methodology to obtain an accurate launch date to minimize Δv. And to validate this proposed methodology, the Psyche mission has been considered as an example, which is discussed in the following sections.

Since the Psyche mission was selected, a variety of changes have occurred, including the development of a new trajectory to support an earlier 2022 lunch opportunity. This paper uses the differential evolution optimization approach and Lambert's problem solution to describe a new launch opportunity and necessary thrust impulse. Section 2 presents the basic description of the differential evolution algorithm (DEA). Section 3 gives the formulation of the analytic calculation of the maneuver thrust impulse and gravity impulse during gravity assist. The proposed methodology process with full details is given in Section 4. Section 5 describes the mission implantation in numerical solution further, Section 5.1 describes the numerical calculation of Earth to Psyche mission. Section 5.2 provides the evaluated numerical data of Psyche to Earth return mission and the Section 6 outlines the conclusion.

2. Differential evolution algorithm

The differential evolution algorithm (DEA) is the most frequently used population-based optimization technique, which is approximately similar to the genetic algorithm. And similar operators are used in DEA like selection, mutation and crossover [7]. The initial population is randomly generated and then evaluated, like any other evolutionary algorithm. It is a straightforward and effective optimizer, particularly for continuous optimization. The DEA uses a self-adaptive scaling factor that is connected to the value of the last generation's fitness function, the number of generations, and a mutation factor to prevent locally optimal solutions. The DEA structure has certain restrictions in the search logic since it comprises a too-small range of exploration actions. This characteristic has prompted several computer scientists to enhance DEA by suggesting changes to the original algorithm. The working principles and the application of the proposed DEA-based methodology have been discussed throughout this paper.

The main steps of the DEA are given the Algorithm 1:

Algorithm 1 : Process of differential evolution algorithm

Require: *the population Initialization*
  call *Evolution*
  while *optimal value* > *tolerance* **do**
    call *Mutation*
    call *Crossover*
    call *Evolution*
    call *Selection*
  end while

When the next number of generations doesn't improve the global optimal solution, or the maximum number of generations G^{max} is reached, then the DEA process stop searching.

2.1. Population initialization

Generally, each decision variable is assigned a randomly chosen real value from its feasible bounds:

$$x_{j,pop}^{(0)} = x_j^{min} + \mu_j(x_j^{max} - x_j^{min}), \quad pop = 1, \ldots, P; \quad j = 1, \ldots, D, \tag{2.1}$$

where $\mu_j \in [0,\ 1]$ is a uniformly distributed random number, generated a new for each value of j. And x_j^{min} and x_j^{max} are the lower and upper bounds of the j^{th} decision variable, respectively.

2.2. Mutation

The mutation operator makes mutant vectors x_{pop} as given below [13]:

$$x'^{(G)}_{pop} = x_l^{(G)} + \beta(x_m^{(G)} - x_n^{(G)}), \quad pop = 1, \ldots, P, \tag{2.2}$$

where x_l, x_m and x_n are randomly chosen vectors among the P population, and $l \neq m \neq n$. x_l, x_m and x_n are selected a new for each parent vector. β is the scaling constant, that is used to improve algorithm convergence. And it also adjusts the perturbation size in the mutation operator.

2.3. Crossover

The crossover operator makes trial vectors x''_{pop} by using the units of the parent vectors x_{pop} and its mutant vectors x'_{pop}, as indicated by the below equation [13]:

$$x''^{(G)}_{j,pop} = \begin{cases} x'^{(G)}_{j,pop}, & \text{if } \alpha_j \leq C_R, \text{ or } j = q; \\ x^{(G)}_{j,pop}, & \text{otherwise;} \end{cases} \tag{2.3}$$
$$pop = 1, \ldots, P; \quad j = 1, \ldots, D,$$

where $\alpha_j \in [0,\ 1]$ is a uniformly distributed random number, generated a new for each value of j. The crossover constant C_R is an algorithm parameter. It aids the algorithm to escape from local minima and controls the diversity of the population. $q \in \{1, \ldots, P\}$ is a randomly chosen index. It guarantees that the trial vector gets at least one unit from the mutant vector.

2.4. Selection

The selection operator, select a vector between the parent vectors $x_{pop}^{(G)}$ and trial vectors $x''^{(G)}_{pop}$, on the basis of their fitness value. It is chosen for the next generation according to the following criteria.

$$x_{pop}^{(G+1)} = \begin{cases} x''^{(G)}_{pop}, & \text{if } x''^{(G)}_{pop} \leq x_{pop}^{(G)}; \\ \\ x_{pop}^{(G)}, & \text{otherwise;} \end{cases} \tag{2.4}$$
$$pop = 1, \ldots, P.$$

This optimization process is rehashed for several generations, permitting individuals to improve their fitness as they explore the solution space in search of optimal values.

The population size P, the crossover constant $C_R \in [0,\ 1]$ and the scaling factor $\beta \in [0,\ 2]$ are three essential control parameters of DEA. The population size determines the number of individuals in the population and provides the algorithm enough diversity to search the solution space. The diversity of the population is controlled by crossover constant. And the amount of perturbation in the mutation process is controlled by the scaling factor.

3. Thrust and gravity impulse

Let's consider that the time spent in gravity assist isn't taken into account. The velocity of the spacecraft in relative to the P_2 is $\vec{v}_\infty$, and its magnitude is v_∞ is given as follow:

$$\sin\left(\frac{\alpha}{2}\right) = \frac{\mu_p/r_f}{v_\infty^2 + \mu_p/r_f}, \tag{3.1}$$

where the α is turning angle, μ_p is the gravitational parameter of the planet and r_f is the flyby radius.

The thrust impulse is defined as the sum of the magnitudes of velocity differences between the arrival velocity (v_-) and the respective departure velocity (v_+). When the gravity assist effect is taken into account, the thruster does not always have the value $|v_+ - v_-|$. As a consequence, the issue that emerges is how to measure the net maneuver impulse analytically. Since

$$v_+ = v_- + \Delta v, \tag{3.2}$$

labeling the gravity assist impulse by Δv_G and thrust impulse by Δv_T. Then

$$\Delta v = \Delta v_G + \Delta v_T, \tag{3.3}$$

the goal of this methodology is to determine the Δv_G where Δv_T is minimal.

As a consequence, after gravity assists, the hyperbolic excess velocity assumes this shape as follow:

$$\vec{v}_{\infty+} = \vec{v}_+ - \vec{v}_p. \tag{3.4}$$

Assume the $\vec{v}_{\infty-}$ in terms of turning angle α, it represented as:

$$\vec{v}_{\infty-} = v_\infty \cdot (\sin\alpha\cos\theta \cdot \vec{k} + \sin\alpha\sin\theta \cdot \vec{j} + \cos\alpha \cdot \vec{i}), \tag{3.5}$$

where

$$v_\infty = |\vec{v}_{\infty+}|, \tag{3.6}$$

$$\vec{j} = \vec{k} \times \vec{i} \text{ and } \vec{k} \perp \vec{i}, \tag{3.7}$$

$$\vec{i} = \frac{\vec{v}_{\infty+}}{v_\infty}, \tag{3.8}$$

$$\alpha \in [0, \alpha_{max}], \tag{3.9}$$

$$\theta \in [0, 2\pi]. \tag{3.10}$$

The α_{max} can be calculated by replacing r_f with r_{min} and is given by

$$\alpha_{max} = 2\sin^{-1}\Big(\frac{1}{v_\infty^2 \frac{r_{min}}{\mu_p} + 1}\Big). \tag{3.11}$$

The unit vector $\vec{k}$ is not unique since it is perpendicular to the unit vector $\vec{i}$. As a result, the only rational solution is provided by

$$\vec{k} = \begin{cases} [i_3, 0, -i_1]^T; |i_2| \le \min(|i_1|, |i_3|), \\ [-i_2, i_1, 0]^T; |i_3| \le \min(|i_1|, |i_2|), \\ [0, -i_3, i_2]^T; |i_1| \le \min(|i_2|, |i_3|), \end{cases} \tag{3.12}$$

where i_1, i_2, i_3 are the directional component of the unit vector $\vec{i}$ respectively. Then the gravity impulse is represented as:

$$\Delta v_G = \vec{v}_{\infty+} - \vec{v}_{\infty-} \tag{3.13}$$

$$= -v_\infty \cdot (\sin\alpha\cos\theta \cdot \vec{k} + \sin\alpha\sin\theta \cdot \vec{j} + (\cos\alpha - 1) \cdot \vec{i}). \tag{3.14}$$

Let's project $\vec{v}_+ - \vec{v}_-$ onto the frame with base vectors i, j, k and divide each part by $v_\infty -$, then it yields

$$\vec{v}_+ - \vec{v}_- = -v_\infty \cdot (x_1 \cdot \vec{i} + x_2 \cdot \vec{j} + x_3 \cdot \vec{k}), \tag{3.15}$$

where

$$x_1 = -\frac{(v_+ - v_-)}{v_\infty} \cdot \vec{i}, \quad x_2 = -\frac{(v_+ - v_-)}{v_\infty} \cdot \vec{j}, \quad x_3 = -\frac{(v_+ - v_-)}{v_\infty} \cdot \vec{k}.$$

From Eqs 3.2, 3.3, 3.14 and 3.15 minimizing $|\Delta v_T|$, i.e., $|v_+ - v_- - \Delta v_G|$ is equivalent to minimizing the function:

$$\frac{|v_+ - v_- - \Delta v_G|^2}{v_\infty^2} = (\sin\alpha\cos\theta - x_3)^2 + (\sin\alpha\sin\theta - x_2)^2 + (\cos\alpha - 1 - x_1)^2, \tag{3.16}$$

where $\alpha \in [0, \alpha_{max}]$ and $\theta \in [0, 2\pi]$ have yet to be discovered. It's not difficult to get to the point where Eq 3.16 is minimal.

$$\alpha = \min(\alpha_{max}, \beta), \quad \theta = \arctan 2(x_2, x_3),$$

where

$$\beta = \cos^{-1}\Big(\frac{1 + x_1}{\sqrt{(1 + x_1)^2 + x_2^2 + x_3^2}}\Big),$$

the four quadrant inverse tangent function is called arctan $2(y, x)$.

Thus, the flyby radius r_f and the corresponding gravity assist impulse that result in minimal thrust impulse can be determined analytically for each pair of arrival velocity $\vec{v}_-$ and departure velocity $\vec{v}_+$.

4. Methodology

A Hohmann transfer is a specific form of lowest fuel transfer orbit for an interplanetary mission. In reality, the Hohmann transfer takes just a little amount of starting fuel to reach the distant planet. It is frequently used to go from one circular orbit to another [19]. As a result, it is an appealing alternative for constructing future expeditions from Earth to Psyche. However, the Hohmann transfer necessitates a 180-degree change in the true anomaly and only offers a rough approximation of how to reach Psyche. A more accurate solution to interplanetary transfer is the patched-conic approximation. It entails breaking down the total transfer into several two-body problems. This approximation, as opposed to the analytic Hohmann solution, gives a far better understanding of the relationship between the departure orbit and the total transfer.

Further, the Lambert's problem is a way to solve for the trajectory connecting two position vectors with a given time of flight. The $\vec{r_0}$ be the initial position vector at the time t_0 and $\vec{r_f}$ be the final position vector at the time t_f. $\Delta t = t_f - t_0$ be the transfer time of the spacecraft between the two positions. The solution of Lambert's problem calculated from the general form Kepler's equation, is defined in Eq 4.1 [3]:

$$t_f - t_0 = \Delta t = \sqrt{\frac{a^3}{\mu}}\Big[2\pi k + (E_f - e\sin E_f) + (E_0 - e\sin E_0)\Big], \tag{4.1}$$

where $E,\ t,\ a,\ e$ and μ are the eccentric anomaly, time, semi-major axis, eccentricity and gravitational parameter respectively. The subscripts "0" and "f" denote the initial and final states respectively, k is an integer number refers to the number of staggering.

Furthermore, we need a technique for determining a minimal fuel transfer orbit for an interplanetary mission from Earth to Psyche. In this regard, we have designed a new methodology with the combination of DEA, Lambert's problem and gravity assists, to achieve this goal. The flow chart of this methodology is given in Figure 1, and the objective function of the DEA is defined as:

$$\text{Obj. Fun.} = \Delta v_1 + \Delta v_T + \Delta v_3. \tag{4.2}$$

The simulation time depends on the size of the data file like 'earth.dat', 'mars.dat' and 'psyche.dat'. In our case, we have collected 3yr, 4yr and 5yr position and velocity data of the Earth, Mars and Psyche respectively with time step 1 minute. In our desktop computer, it takes 3–5 seconds to calculate the optimal opportunity. We run this code up to 100 repetitions to calculate the average simulation time, which is 4 seconds. The Python interpreted language has been used to code the whole algorithm.

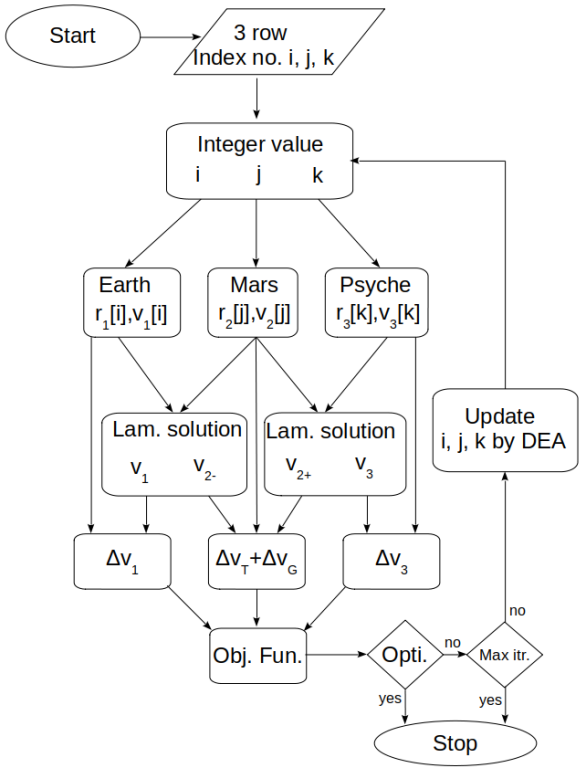

Figure 1. Flow chart of the methodology simulation process.

So, the last iterated value of this process gives us the optimal launch, flyby and arrival date. The approach may converge on a physically reasonable solution on every simulation, and only a few simulation runs are necessary to gain confidence in the strength of the best solution. The degree of resilience was achieved with the most basic DEA capabilities and significant constraints on the fitness function's ability to assess a valuable class of trajectories. The approach, while functional, may benefit from some enhancements to allow for improved searching and result refining. It has been found that repopulating a segment of certain generations on a regular basis might assist in potentially avoiding local minimums while reducing the number of low population simulations necessary.

5. Numerical simulation and discussion

As previously mentioned, the future Psyche mission will be used as a case study for numerical simulation. The technique and hypotheses have discussed in Sections 2 and 3. All computations are performed on a desktop with a 3.5 GHz processor and 16 GB of RAM-memory. The heliocentric position and velocity of planets and asteroid, and their date and period have been collected from the Jet Propulsion Laboratory (JPL) horizons system.

5.1. Earth to Psyche opportunity

The problem of getting transfer trajectory from Earth to Psyche with the aid of Mars's gravity is considered. The spacecraft departs from Earth's heliocentric position and arrives at the heliocentric position of Psyche asteroid. The example is exactly same as that of in the article [22]. To start the

evolution, three separate data files of Earth, Mars and Psyche are collected from JPL Horizon. Each file contains total 7 columns, column 1 denotes the epoch time, the next 3 columns give the positions and the next 3 columns give velocities. The row index number of all data files are assumed as the variable for DEA. The objective function is described in Eq 4.2, with goal to minimize the required Δv. The optimal launch, flyby and arrival epoch have been calculated by DEA optimization and described in Table 2. All constants are given in Table 3.

Table 2. All calculated data of Psyche mission.

Parameter	Value	Units
Initial time	2022-08-16 15:37	Coordinate time
Initial position	[1.20297254e+08, -9.00620125e+07, 3.40254165e+04]	km.
Initial velocity	[1.72676218e+01, 2.37833963e+01, -2.10769603e-03]	km./sec.
Flyby time	2023-07-01 12:23	Coordinate time
Flyby position	[-2.45888470e+08, 4.30296234e+07, 6.93820194e+06]	km.
Flyby velocity	[-3.30914219, -21.80549084, -0.37539658]	km./sec.
Arrival time	2025-04-27 16:07	Coordinate time
Arrival position	[3.56039705e+08, 1.24777765e+08, -1.55076566e+07]	km.
Arrival velocity	[-6.63897994, 18.780373, -0.70081359]	km./sec.
Transfer time	985.020833	days

Table 3. All important constants.

Parameter	Value	Units
Mars radius	3389.50	km.
Mars Gravitational parameter	42828.3744	$km.^3/sec^2$
Sun Gravitational parameter	$1.32712442 \cdot e^{+11}$	$km.^3/sec^2$

In the evolution process, Lambert's problem being solved continuously two times from Earth to Mars and Mars to Psyche respectively. The first solution gives the spacecraft Earth departure and Mars arrival velocities. To obtain Δv_1, the Earth velocity is subtracted from spacecraft departure velocity. Again we solve Lambert's problem from Mars to Psyche and get the spacecraft velocity vectors at Mars and Psyche. To obtain Δv_3, we subtracted the Psyche velocity from spacecraft velocity. On Mars, there are two impulses act on the spacecraft. One is the maneuver thrust impulse and the other is gravity impulse. The sum of these two impulses is the total maneuver impulse Δv_2, which is required to transfer a spacecraft to the Psyche.

Furthermore, the inbound and outbound legs at Mars have already been calculated . The next step for obtaining the maneuver thrust is to calculate the optimal flyby radius, which fulfills our aim, that is to get the maximum gravity impulse with the least thrust impulse. The calculated optimal flyby radius is $r_f = 3491.9\ km$ for this mission.

Besides, to calculating the total maneuver impulse (Δv_2) as defined in Eq 3.3, we follow the algorithm process of Section 3. We consider $r_{min} = 3489.9\ km$ and start the optimization. The calculated values are represented in Table 4.

Table 4. Computed optimal impulse of the mission.

Flyby radius ($km.$)	Δv_1	Δv_2		Δv_3	Total impulse ($\frac{km.}{sec}$)	Comp. time
		Δv_T	Δv_G		$\Delta v_1+\Delta v_T+\Delta v_3$	($sec.$)
3491.9	4.555484	3.308965	2.121037	3.471180	11.335629	3.4

The spacecraft trajectory portrays in Figure 2(a). In this figure, blue, green and gray orbits represent the orbit of Earth, Mars and Psyche respectively. The red color arc represents the transfer trajectory using Mars gravity assists. The blue dot is the Earth's departure position. Green dot is the Mars's position at the flyby time and the red dot is Psyche's position at arrival time. Figure 2(b) demonstrates the spacecraft velocity for the whole transfer time.

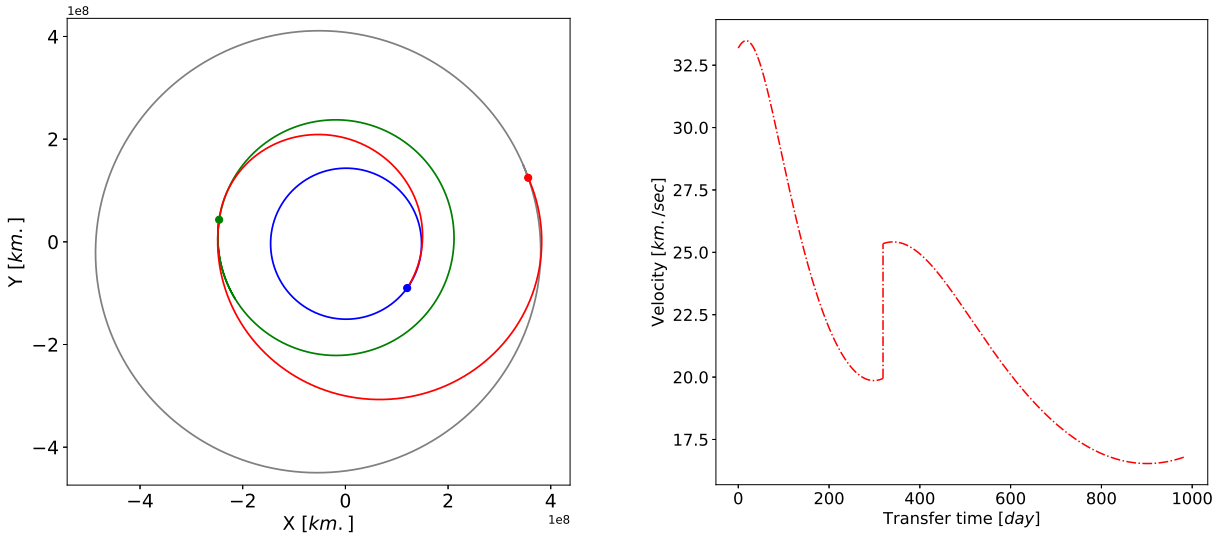

(a) (b)

Figure 2. Transfer trajectory and spacecraft velocity.

5.2. Psyche to Earth opportunity

The spacecraft analyses the asteroid from their parking orbit and collects asteroid physical samples. It will begin its return journey to Earth after 1710 solar days (4.68 years). The problem of getting trajectory solution from Psyche to Earth using Mars gravity assists is discussed. The spacecraft departs from Psyche's heliocentric position and arrives at the heliocentric position of Earth. To start the evolution, three separated new data files of Psyche, Mars and Earth is collected JPL Horizon of later epoch. The optimal launch, flyby and arrival epoch have been evaluated by DEA optimization and described in Table 5. For this mission, the calculated optimal flyby radius is $r_f = 4234.31206\ km$. The calculated value of impulses are represented in Table 6.

Table 5. All calculated data of Earth return mission.

Parameter	Value	Units
Initial time	2030-01-01 01:07	Coordinate time
Initial position	[3.76301980e+08, -7.22865866e+07, -6.80964928e+06]	km.
Initial velocity	[2.06594109, 14.35277651, 0.21905743]	km./sec.
Flyby time	2031-06-25 05:17	Coordinate time
Flyby position	[-7.70438786e+07, -2.10799322e+08, -2.52815573e+06]	km.
Flyby velocity	[18.58929317, -16.57062545, -0.05647533]	km./sec.
Arrival time	2033-02-17 19:48	Coordinate time
Arrival position	[-1.27430790e+08, 7.60491308e+07, 1.60787188e+04]	km.
Arrival velocity	[-18.49064939, -29.73439814, -0.40061276]	km./sec.
Transfer time	1143.792502	days

Table 6. Computed optimal impulse of the return mission.

Flyby radius ($km.$)	Δv_1	Δv_2		Δv_3	Total impulse ($\frac{km.}{sec}$)	Comp. time
		Δv_T	Δv_G		$\Delta v_1+\Delta v_T+\Delta v_3$	($sec.$)
4234.31206	5.349698	1.664216	0.141844	4.893526	11.907440	4.1

The spacecraft trajectory portrays in Figure 3(a). In this figure, gray, green and blue orbits represent the orbit of Psyche, Mars and Earth respectively. The red color arc represents the transfer trajectory using Mars gravity assist. The blue dot is the Psyche's departure position. Green dot represents the Mars's position at the flyby time and the red dot represents Earth's position at arrival time. Figure 3(b) portrays the spacecraft velocity for the whole transfer time.

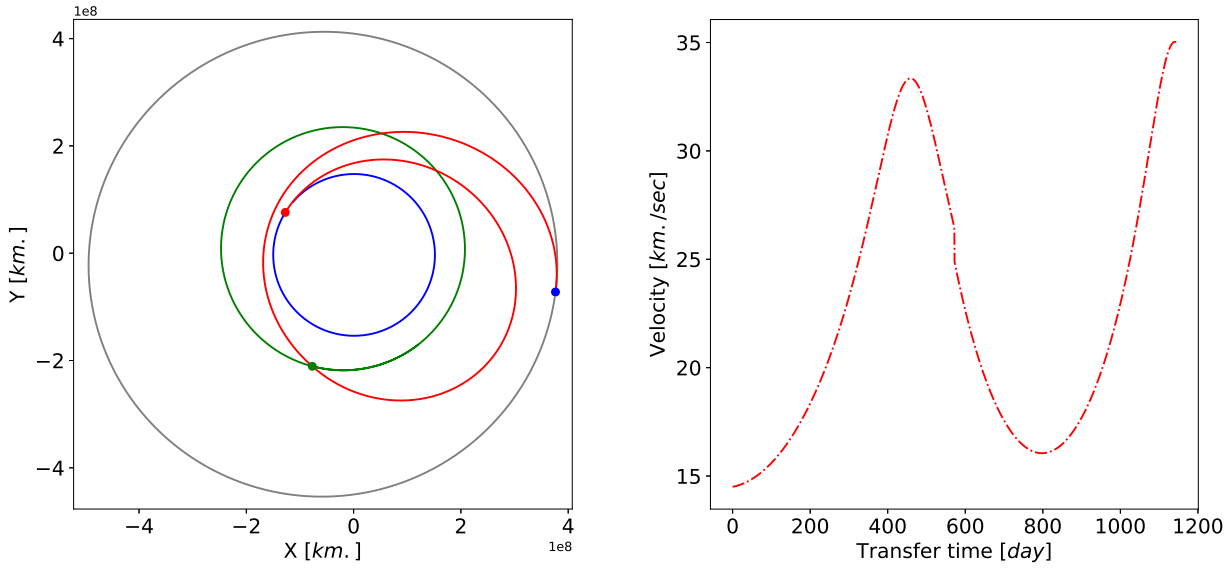

(a) (b)

Figure 3. Transfer trajectory and spacecraft velocity.

6. Conclusions

In this work, a new opportunity to Psyche mission with Mars's gravity assists is presented. The DEA is used as the outer layer optimizer, setting the parameter as the row index number of three data files. Whereas an inner layer, Lambert's problem is used to find the feasible trajectory of the rendezvous problem. This methodology show promise as a rapid low fidelity tool to find optimal transfer trajectories. Many kinds of literature show, the actual Psyche mission will take 1277±15 days to reach near the Psyche asteroid, and there is no solution for return to the Earth. In our calculation, the Psyche journey took only 985±21 days. And the return opportunity has also calculated with a journey time of 1143±13 days. The result shows that the spacecraft required only three thrust impulses, Δv_1, Δv_T and Δv_3 at departure, flyby and arrival positions respectively. Both elliptic and hyperbolic transfers may be handled using the suggested approach. In addition, the proposed approach provides high accuracy and a faster speed to get the optimal launch opportunities. Future work focuses on expanding this technique to high fidelity environments and tighter arrival tolerance to build the methodology further.

Conflict of interest

The authors declare no conflicts of interest.

References

1. J. D. Anderson, P. A. Laing, E. L. Lau, A. S. Liu, M. M. Nieto, S. G. Turyshev, Study of the anomalous acceleration of Pioneer 10 and 11, *Phys. Rev. D*, **65** (2002), 082004. https://doi.org/10.1103/PhysRevD.65.082004
2. R. Armellin, D. Gondelach, J. F. San Juan, Multiple revolution perturbed Lambert problem solvers, *J. Guid. Control Dynam.*, **41** (2018), 2019–2032. https://doi.org/10.2514/1.G003531
3. R. H. Battin, Lambert's problem revisited, *AIAA J.*, **15** (1977), 707–713. https://doi.org/10.2514/3.60680
4. R. H. Battin, *An introduction to the mathematics and methods of astrodynamics*, Reston, Virginia: AIAA, 1999.
5. E. R. Lancaster, R. C. Blanchard, R. A. Devaney, A note on Lambert's theorem, *J. Spacecraft Rockets*, **3** (1966), 1436–1438.
6. D. Brownlee, The stardust mission: Analyzing samples from the edge of the solar system, *Annu. Rev. Earth Pl. Sci.*, **42** (2014), 179–205. https://doi.org/10.1146/annurev-earth-050212-124203
7. U. K. Chakraborty, *Advances in differential evolution*, Berlin, Heidelber: Springer, 2008. https://doi.org/10.1007/978-3-540-68830-3
8. W. Hart, G. M. Brown, S. M. Collins, M. D. S. S. Pich, P. Fieseler, D. Goebel, et al., Overview of the spacecraft design for the Psyche mission concept, In: *2018 IEEE Aerospace Conference*, 2018, 1–20. https://doi.org/10.1109/AERO.2018.8396444
9. D. Izzo, Revisiting Lambert's problem, *Celest. Mech. Dyn. Astr.*, **121** (2015), 1–15. https://doi.org/10.1007/s10569-014-9587-y

10. V. Kumar, B. S. Kushvah, Computation of periodic orbits around L_1 and L_2 using PSO technique, *Astron. Rep.*, **64** (2020), 82–93. https://doi.org/10.1134/S1063772920010059

11. D. S. Lauretta, S. S. Balram-Knutson, E. Beshore, W. V. Boynton, C. D. D'Aubigny, D. N. DellaGiustina, et al., Osiris-rex: Sample return from asteroid (101955) Bennu, *Space Sci. Rev.*, **212** (2017), 925–984. https://doi.org/10.1007/s11214-017-0405-1

12. Z. Q. Luo, G. M. Dai, L. Peng, A novel model for the optimization of interplanetary trajectory using evolutionary algorithm, *J. Comput.*, **6** (2011), 2243–2248.

13. D. Marsh, J. Catchen, V. Sereno, D. Trofimov, Evolution of the preliminary fault management architecture and design for the Psyche mission, In: *2020 IEEE Aerospace Conference*, 2020, 1–15. https://doi.org/10.1109/AERO47225.2020.9172741

14. M. G. Martin, W. A. Hoey, J. M. Alred, C. E. Soares, Novel contamination control model development and application to the Psyche asteroid mission, In: *2020 IEEE Aerospace Conference*, 2020, 1–9. https://doi.org/10.1109/AERO47225.2020.9172321

15. M. Meltzer, Mission to Jupiter: A history of the Galileo project, *NASA STI/Recon Tech. Rep. N*, **7** (2007), 13975.

16. D. Y. Oh, D. M. Goebel, L. Elkins-Tanton, C. Polanskey, P. Lord, S. Tilley, et al., Psyche: Journey to a metal world, In: *52nd AIAA/SAE/ASEE Joint Propulsion Conference*, 2016. https://doi.org/10.2514/6.2016-4541

17. V. S. Özsoy, M. G. Ünsal, H. H. Örkcü, Use of the heuristic optimization in the parameter estimation of generalized gamma distribution: Comparison of GA, DE, PSO and SA methods, *Computation. Stat.*, **35** (2020), 1895–1925. https://doi.org/10.1007/s00180-020-00966-4

18. L. Peng, Y. Z. Wang, G. M. Dai, Y. M. Chang, F. J. Chen, Optimization of the Earth-Moon low energy transfer with differential evolution based on uniform design, In: *IEEE Congress on Evolutionary Computation*, 2010, 1–8. https://doi.org/10.1109/CEC.2010.5586384

19. J. E. Prussing, Simple proof of the global optimality of the Hohmann transfer, *J. Guidance*, **15** (1992), 1037–1038. https://doi.org/10.2514/3.20941

20. M. D. Rayman, T. C. Fraschetti, C. A. Raymond, C. T. Russell, Dawn: A mission in development for exploration of main belt asteroids Vesta and Ceres, *Acta Astronaut.*, **58** (2006), 605–616. https://doi.org/10.1016/j.actaastro.2006.01.014

21. H. Schaub, J. L. Junkins, *Analytical mechanics of space systems*, Reston, Virginia: AIAA, 2003.

22. J. A. Sims, *Delta-V gravity-assist trajectory design: Theory and practice*, Purdue University, 1996.

23. J. S. Snyder, V. H. Chaplin, D. M. Goebel, R. R. Hofer, A. Lopez Ortega, I. G. Mikellides, et al., Electric propulsion for the Psyche mission: Development activities and status, In: *AIAA Propulsion and Energy 2020 Forum*, 2020. https://doi.org/10.2514/6.2020-3607

24. J. S. Snyder, D. M. Goebel, V. Chaplin, A. L. Ortega, I. G. Mikellides, F. Aghazadeh et al., Electric propulsion for the Psyche mission, In: *36th International Electric Propulsion Conference*, 2019.

25. Y. Tsuda, M. Yoshikawa, T. Saiki, S. Nakazawa, S. I. Watanabe, Hayabusa2-sample return and kinetic impact mission to near-earth asteroid Ryugu, *Acta Astronaut.*, **156** (2019), 387–393. https://doi.org/10.1016/j.actaastro.2018.01.030

26. M. Vasile, P. De Pascale, Preliminary design of multiple gravity-assist trajectories, *J. Spacecraft Rockets*, **43** (2006), 794–805. https://doi.org/10.2514/1.17413

27. S. Wagner, B. Wie, Hybrid algorithm for multiple gravity-assist and impulsive Delta-V maneuvers, *J. Guidance*, **38** (2015), 2096–2107. https://doi.org/10.2514/1.G000874

28. G. Whiffen, Mystic: Implementation of the static dynamic optimal control algorithm for high-fidelity, low-thrust trajectory design, In: *AIAA/AAS Astrodynamics Specialist Conference and Exhibit*, 2006. https://doi.org/10.2514/6.2006-6741

29. Z. Yang, Y. Z. Luo, J. Zhang, G. J. Tang, Homotopic perturbed Lambert algorithm for long-duration rendezvous optimization, *J. Guidance*, **38** (2015), 2215–2223. https://doi.org/10.2514/1.G001198

30. M. Yoshikawa, J. Kawaguchi, A. Fujiwara, A. Tsuchiyama, Hayabusa sample return mission, In: *Asteroids IV*, Tucson: University of Arizona, 2015, 397–418. https://doi.org/10.2458/azu_uapress_9780816532131-ch021

31. X. Zeng, Z. Liu, W. J. Fu, F. Zhao, Application of improved differential evolution algorithm in reactive power optimization, *Power Syst. Tech.*, **2** (2012), 121–125.

32. G. Zhang, Terminal-velocity-based Lambert algorithm, *J. Guidance*, **43** (2020), 1529–1539. https://doi.org/10.2514/1.G004964

33. G. Zhang, D. Zhou, D. Mortari, Optimal two-impulse rendezvous using constrained multiple-revolution Lambert solutions, *Celest. Mech. Dyn. Astr.*, **110** (2011), 305–317. https://doi.org/10.1007/s10569-011-9349-z

34. G. Zhang, D. Zhou, D. Mortari, M. R. Akella, Covariance analysis of Lambert's problem via Lagrange's transfer-time formulation, *Aerosp. Sci. Technol.*, **77** (2018), 765–773. https://doi.org/10.1016/j.ast.2018.03.039

35. M. C. Zuo, G. M. Dai, L. Peng, Z. Tang, A differential evolution-based optimization tool for interplanetary transfer trajectory design, *arXiv Preprint*, 2021. Available from: `https://arxiv.org/abs/2011.06780`.

AIMS Press